Inorganic Chemistry
Article

Inorg. Chem. **2010**, *49*, 9617–9626 **9617**
DOI: 10.1021/ic101278w

From Infinite One-Dimensional Helix to Discrete Cu^{II}_{15} Cluster along with in Situ S_N2 Ring-Cleavage of *cis*-Epoxysuccinic Acid: pH-Controlled Assemblies, Crystal Structures, and Properties

Shao-Ming Fang,[†] Qiang Zhang,[†] Min Hu,[†] E. Carolina Sañudo,*[,§] Miao Du,*[,‡] and Chun-Sen Liu*[,†]

[†]*Zhengzhou University of Light Industry, Henan Provincial Key Laboratory of Surface & Interface Science, Zhengzhou, Henan 450002, P.R. China,* [‡]*College of Chemistry, Tianjin Key Laboratory of Structure and Performance for Functional Molecule, Tianjin Normal University, Tianjin 300387, P.R. China, and* [§]*Institut de Nanociència i Nanotecnologia i Departament de Química Inorgànica, Universitat de Barcelona, Diagonal, 647, 08028-Barcelona, Spain*

Received June 27, 2010

Two Cu^{II} coordination complexes $\{[Cu(ces)(H_2O)_2](H_2O)_{0.5}\}_n$ (**1**) and $[Cu_{15}(dhs)_6(OH)_6(H_2O)_{10}](H_2O)_{20}$ (**2**) have been synthesized from *cis*-epoxysuccinic acid (*cis*-H_2ces) and Cu^{II} perchlorate under different pH conditions (ces = *cis*-epoxysuccinate and dhs = 2,3-dihydroxysuccinate), and fully characterized by IR spectra, elemental analyses, as well as single crystal and powder X-ray diffraction techniques. Notably, when the reaction was performed at pH above about 7.4, a one-dimensional (1-D) helical chain complex **1** is formed, whereas a neutral isolated Cu_{15} nanocluster **2** is generated when the pH value is decreased to the range of about 6.6−7.3, being concomitant with in situ S_N2 ring-cleavage reaction of *cis*-H_2ces to form (2*S*,3*S*)- and (2*R*,3*R*)-H_4dhs. Further, extended supramolecular architectures are constructed via secondary interactions in both structures. The magnetic properties of **1** and **2** have also been studied in detail, showing that **1** is an antiferromagnetic helical chain of $S = 1/2$ spins and **2** possesses an $S = 3/2$ spin ground state.

Introduction

Recently, the realm of crystal engineering has been flourishing, and crystal-engineering techniques are widely used for design and synthesis of multifarious functional crystalline materials.[1−4] The construction of helical coordination polymers[5] and polynuclear 3d transition-metal (TM) clusters[6] have attracted particular interest not only because of

*To whom correspondence should be addressed. E-mail: chunsenliu@zzuli.edu.cn (C.-S.L.), dumiao@public.tpt.tj.cn (M.D.), carolina.sanudo@qi.ub.es (E.C.S.).

(1) For some reviews, please see: (a) Batten, S. R.; Robson, R. *Angew. Chem., Int. Ed.* **1998**, *37*, 1460. (b) Katritzky, A. R.; Nichols, D. A.; Siskin, M.; Murugan, R.; Balasubramanian, M. *Chem. Rev.* **2001**, *101*, 837. (c) Férey, G. *Chem. Soc. Rev.* **2008**, *37*, 191. (d) Cundy, C. S.; Cox, P. A. *Chem. Rev.* **2003**, *130*, 663. (e) Janiak, C. *Dalton Trans.* **2003**, 2781. (f) James, S. L. *Chem. Soc. Rev.* **2003**, *32*, 276. (g) Zhang, J. P.; Huang, X. C.; Chen, X. M. *Chem. Soc. Rev.* **2009**, *38*, 2385. (h) Moulton, B.; Zaworotko, M. J. *Chem. Rev.* **2001**, *101*, 1629. (i) Eddaoudi, M.; Moler, D. B.; Li, H.; Chen, B.; Reineke, T.; O'Keeffe, M.; Yaghi, O. M. *Acc. Chem. Res.* **2001**, *34*, 319. (j) Vittal, J. J. *Coord. Chem. Rev.* **2007**, *251*, 1781. (k) Morris, R. E.; Bu, X. *Nat. Chem.* **2010**, *2*, 353.

(2) (a) Wang, B.; Coté, A. P.; Furukawa, H.; O'Keeffe, M.; Yaghi, O. M. *Nature* **2008**, *453*, 207. (b) Zhang, J.-P.; Kitagawa, S. *J. Am. Chem. Soc.* **2008**, *130*, 907. (c) Férey, G.; Serre, C. *Chem. Soc. Rev.* **2009**, *38*, 1380. (d) Zhao, D.; Yuan, D. Q.; Zhou, H. C. *Energy Environ. Sci.* **2008**, *1*, 222. (e) Bradshaw, D.; Prior, T. J.; Cussen, E. J.; Claridge, J. B.; Rosseinsky, M. J. *J. Am. Chem. Soc.* **2004**, *126*, 6106. (f) Gao, S. Y.; Yuan, D. Q.; Lu, J.; Li, T. H.; Cao, R. *Chem. Commun.* **2007**, 1813. (g) Wu, D. Y.; Sato, O.; Einaga, Y.; Duan, C. Y. *Angew. Chem., Int. Ed.* **2009**, *48*, 1475. (h) Bu, X. H.; Tong, M. L.; Chang, H. C.; Kitagawa, S.; Batten, S. R. *Angew. Chem., Int. Ed.* **2004**, *43*, 192. (i) Wang, M. S.; Guo, G. C.; Zou, W. Q.; Zhou, W. W.; Zhang, Z. J.; Xu, G.; Huang, J. S. *Angew. Chem., Int. Ed.* **2008**, *47*, 3565. (j) Zeng, M.-H.; Wang, Q.-X.; Tan, Y.-X.; Hu, S.; Zhao, H.-X.; Long, L.-S.; Kurmoo, M. *J. Am. Chem. Soc.* **2010**, *132*, 2561.

(3) (a) Zhang, J. P.; Chen, X. M. *J. Am. Chem. Soc.* **2008**, *130*, 6010. (b) Zhao, B.; Chen, X. Y.; Cheng, P.; Liao, D. Z.; Yan, S. P.; Jiang, Z. H. *J. Am. Chem. Soc.* **2004**, *126*, 15394. (c) Zou, R.-Q.; Sakurai, H.; Han, S.; Zhong, R.-Q.; Xu, Q. *J. Am. Chem. Soc.* **2007**, *129*, 8402. (d) Ye, Q.; Song, Y.-M.; Wang, G.-X.; Chen, K.; Fu, D.-W.; Chan, P.-W.; Zhu, J.-S.; Huang, S.-D.; Xiong, R.-G. *J. Am. Chem. Soc.* **2006**, *128*, 6554. (e) Lan, A. J.; Li, K. H.; Wu, H. H.; Olson, D. H.; Emge, T. J.; Ki, W.; Hong, M. C.; Li, J. *Angew. Chem., Int. Ed.* **2009**, *48*, 2334. (f) Wang, X. Y.; Wang, L.; Wang, Z. M.; Gao, S. *J. Am. Chem. Soc.* **2006**, *128*, 674. (g) Chu, Q.; Liu, G.-X.; Huang, Y.-Q.; Wang, X.-F.; Sun, W.-Y. *Dalton Trans.* **2007**, 4302. (h) Lu, J.; Bi, W.-H.; Xiao, F.-X.; Batten, S. R.; Cao, R. *Chem. Asian J.* **2008**, *3*, 542. (i) Jiang, H.-L.; Liu, B.; Akita, T.; Haruta, M.; Sakurai, H.; Xu, Q. *J. Am. Chem. Soc.* **2009**, *131*, 11302.

(4) (a) Tanaka, D.; Henke, A.; Albrecht, K.; Moeller, M.; Nakagawa, K.; Kitagawa, S.; Groll, J. *Nat. Chem.* **2010**, *2*, 410. (b) Li, X. Z.; Li, M. A.; Li, Z.; Hou, J. Z.; Huang, X. C.; Li, D. *Angew. Chem., Int. Ed.* **2008**, *47*, 6371. (c) Lu, W. G.; Su, C. Y.; Lu, T. B.; Jiang, L.; Chen, J. M. *J. Am. Chem. Soc.* **2006**, *128*, 34. (d) Kong, L. Y.; Zhang, Z. H.; Zhu, H. F.; Kawaguchi, H.; Okamura, T.; Doi, M.; Chu, Q.; Sun, W. Y.; Ueyama, N. *Angew. Chem., Int. Ed.* **2005**, *44*, 4352. (e) Guo, Z.-G.; Cao, R.; Wang, X.; Li, H.-F.; Yuan, W.-B.; Wang, G.-J.; Wu, H.-H.; Li, J. *J. Am. Chem. Soc.* **2009**, *131*, 6894. (f) Kong, X.-J.; Wu, Y.-L.; Long, L.-S.; Zheng, L.-S.; Zheng, Z.-P. *J. Am. Chem. Soc.* **2009**, *131*, 6918. (g) Zou, R.-Q.; Sakurai, H.; Xu, Q. *Angew. Chem., Int. Ed.* **2006**, *45*, 2542. (h) Cui, H.; Zhou, B.; Long, L. S.; Okano, Y.; Kobayashi, H.; Kobayashi, A. *Angew. Chem., Int. Ed.* **2008**, *47*, 3376. (i) Su, C.-Y.; Goforth, A. M.; Smith, M. D.; Pellechia, P. J.; zur Loye, H. C. *J. Am. Chem. Soc.* **2004**, *126*, 3576. (j) Hou, H.; Wei, Y.; Song, Y.; Mi, L.; Tang, M.; Li, L.; Fan, Y. *Angew. Chem., Int. Ed.* **2005**, *44*, 6067. (k) Zhang, H.-M.; Li, Y.-G.; Lu, Y.; Clérac, R.; Zhang, Z.-M.; Wu, Q.; Feng, X.-J.; Wang, E.-B. *Inorg. Chem.* **2009**, *48*, 10889. (l) Gu, Z.-G.; Sevov, S. C. *Inorg. Chem.* **2009**, *48*, 8066.

Published on Web 09/20/2010

their architectural beauty but also because of their fascinating chemical and physical properties of fluorescence, magnetism, nonlinear optics (NLO), asymmetric catalysis, and enantiomorph separation.[5,6] The common motif in metal−organic helical structures are single-, double-, and multistranded one-dimensional (1-D) helical chains with right-handed (Δ or *P*), left-handed (Λ or *M*) and *meso*-helices, as well as two-dimensional (2-D) sheets, and three-dimensional (3-D) frameworks containing 1-D helical features.[5] Several excellent reviews and papers have been published recently on this subject.[5a−d] It is worth noting, on the other hand, that several polynuclear Cu^{II} clusters with differently homometallic high-nuclearity have also been reported, for example, Cu_6,[6a−d] Cu_8,[6d−g] Cu_9,[6d] Cu_{10},[6h] Cu_{12},[6d,I,j] Cu_{14},[6d] Cu_{16},[6k] Cu_{21},[6k] Cu_{36},[6l,m] and Cu_{44},[6n] which show discrete cage, wheel, flywheel, cyclic, gridlike, tricorne, and saddlelike structures as well as interesting magnetic, catalytic, and cation-exchange properties.[6]

Chemists commonly take advantage of the assembling processes, by comprehending the information embedded in the metal ions and organic ligands, and then direct the 3-D assemblies in a programmed way.[7] However, achieving any specific target material by coordination-driven assembly is challenging at this stage. Obviously, this uncertainty mainly derives from more than one possibility of metal coordination and ligand connecting as well as interference of secondary interactions,[8] which are usually directed by external physical or chemical stimuli.[9−14] Among them, the pH value is a crucial influence on the existing forms and coordination modes of organic ligands as well as crystallization kinetics, and so on.[14] Especially for polycarboxyl compounds, the pH value may sensitively regulate their deprotonation degrees and charges, which will affect the ligand binding modes and the metal-to-ligand ratios, and thus, the overall crystal structures of the final products. Notably, pH dependent in situ ligand reaction in coordination assemblies still remains rarely explored so far.[9a]

Oxirane-2,3-dicarboxylic acid (also known as epoxysuccinic acid) is commercially valuable as an important intermediate in the production of 2,3-dihydroxysuccinic acid (H_4dhs) (also known as tartaric acid), and displays diverse applications in chemical industry, biochemistry, and pharmaceuticals.[15] In this context, (2*S*,3*R*)-oxirane-2,3-dicarboxylic acid (also known as *cis*-epoxysuccinic acid, *cis*-H_2ces), has two chiral centers in the ternary ring backbone as well as a pair of carboxyl groups, which can be regarded as an interesting building tecton in coordination assemblies. On the one hand, pH medium is able to modulate the deprotonated degrees of carboxyl for *cis*-H_2ces to result in multiform binding fashions with the metal centers. On the other hand, oxirane may also suffer the S_N2 ring-cleavage reaction in alkaline condition, to in situ afford (2*R*,3*R*)- and/or (2*S*,3*S*)-2,3-dihydroxysuccinic acid (H_4dhs), which will facilitate the

(5) (a) Zheng, X.-D.; Lu, T.-B. *CrystEngComm* **2010**, *12*, 324. (b) Han, L.; Hong, M. *Inorg. Chem. Commun.* **2005**, *8*, 406. (c) Nakano, T.; Okamoto, Y. *Chem. Rev.* **2001**, *101*, 4013. (d) Albrecht, M. *Chem. Rev.* **2001**, *101*, 3457. (e) Seo, J. S.; Whang, D.; Lee, H.; Jun, S. I.; Oh, J.; Jeon, Y. J.; Kim, K. *Nature* **2000**, *404*, 982. (f) Lee, S.-J.; Hu, A.-G.; Lin, W.-B. *J. Am. Chem. Soc.* **2002**, *124*, 12948. (g) Kondo, M.; Miyazawa, M.; Irie, Y.; Shinagawa, R.; Horiba, T.; Nakamura, A.; Naito, T.; Maeda, K.; Utsuno, S.; Uchida, F. *Chem. Commun.* **2002**, 2156. (h) Kitagawa, S.; Kitaura, R.; Noro, S. *Angew. Chem., Int. Ed.* **2004**, *43*, 2334. (i) Jiang, L.; Feng, X.-L.; Su, C.-Y.; Chen, X.-M.; Lu, T.-B. *Inorg. Chem.* **2007**, *46*, 2637. (j) Ou, G.-C.; Jiang, L.; Feng, X.-L.; Lu, T.-B. *Inorg. Chem.* **2008**, *47*, 2710. (k) Lu, W.-G.; Gu, J.-Z.; Jiang, L.; Tan, M.-Y.; Lu, T.-B. *Cryst. Growth Des.* **2008**, *8*, 192. (l) Zhang, J.; Chen, S.-M.; Wu, T.; Feng, P.-Y.; Bu, X.-H. *J. Am. Chem. Soc.* **2008**, *130*, 12882. (m) Fang, S.-M.; Zhang, Q.; Hu, M.; Xiao, B.; Zhou, L.-M.; Sun, G.-H.; Gao, L.-J.; Du, M.; Liu, C.-S. *CrystEngComm* **2010**, *12*, 2203.

(6) (a) Liu, X.; McLaughlin, A. C.; de Miranda, M. P.; McInnes, E. J. L.; Kilner, C. A.; Halcrow, M. A. *Chem. Commun.* **2002**, 2978. (b) Afrati, T.; Dendrinou-Samara, C.; Zaleski, C. M.; Kampf, J. W.; Pecoraro, V. L.; Kessissoglou, D. P. *Inorg. Chem. Commun.* **2005**, *8*, 1173. (c) Mohamed, A. A.; Burini, A.; Galassi, R.; Paglialunga, D.; Galán-Mascarós, J.-R.; Dunbar, K. R.; Fackler, J. P., Jr. *Inorg. Chem.* **2007**, *46*, 2348. (d) Mezei, G.; Baran, P.; Raptis, R. G. *Angew. Chem., Int. Ed.* **2004**, *43*, 574. (e) Armentano, D.; Mastropietro, T. F.; Julve, M.; Rossi, R.; Rossi, P.; Munno, G. D. *J. Am. Chem. Soc.* **2007**, *129*, 2740. (f) Ardizzoia, G. A.; Angaroni, M. A.; Monica, G. L.; Cariati, F.; Cenini, S.; Moret, M.; Masciocchi, N. *Inorg. Chem.* **1991**, *30*, 4347. (g) Zhao, J.; Mi, L.; Hu, J.; Hou, H.; Fan, Y. *J. Am. Chem. Soc.* **2008**, *130*, 15222. (h) Chang, C.-H.; Hwang, K. C.; Liu, C.-S.; Chi, Y.; Carty, A. J.; Scoles, L.; Peng, S.-M.; Lee, G.-H.; Reedijk, J. *Angew. Chem., Int. Ed.* **2001**, *40*, 4651. (i) Tangoulis, V.; Raptopoulou, C. P.; Paschalidou, S.; Bakalabassis, E. G.; Perlepes, S. P.; Terzis, A. *Angew. Chem., Int. Ed. Engl.* **1997**, *36*, 1083. (j) Matthews, C. J.; Onions, S. T.; Morata, G.; Salvia, M. B.; Elsegood, M. R. J.; Price, D. J. *Chem. Commun.* **2003**, 320. (k) Bai, Y.-L.; Tangoulis, V.; Huang, R.-B.; Zheng, L.-S.; Tao, J. *Chem.—Eur. J.* **2009**, *15*, 2377. (l) Abedin, T. S. M.; Thompson, L. K.; Miller, D. O.; Krupicka, E. *Chem. Commun.* **2003**, 708. (m) Murugesu, M.; Clérac, R.; Anson, C. E.; Powell, A. K. *Chem. Commun.* **2004**, 1598. (n) Murugesu, M.; Clérac, R.; Anson, C. E.; Powell, A. K. *Inorg. Chem.* **2004**, *43*, 7269.

(7) (a) Cheng, J.-K.; Yao, Y.-G.; Zhang, J.; Li, Z.-J.; Cai, Z.-W.; Zhang, X.-Y.; Chen, Z.-N.; Chen, Y.-B.; Kang, Y.; Qin, Y.-Y.; Wen, Y.-H. *J. Am. Chem. Soc.* **2004**, *126*, 7796. (b) Hu, K. L.; Kurmoo, M.; Wang, Z. M.; Gao, S. *Chem.—Eur. J.* **2009**, *15*, 12050. (c) Wang, J.; Lin, Z.-J.; Ou, Y.-C.; Yang, N.-L.; Zhang, Y.-H.; Tong, M.-L. *Inorg. Chem.* **2008**, *47*, 190. (d) Natarajan, S.; Mahata, P. *Chem. Soc. Rev.* **2009**, *38*, 2304. (e) Du, M.; Zhang, Z.-H.; Tang, L.-F.; Wang, X.-G.; Zhao, X.-J.; Batten, S. R. *Chem.—Eur. J.* **2007**, *13*, 2578.

(8) (a) Ye, B.-H.; Tong, M.-L.; Chen, X.-M. *Coord. Chem. Rev.* **2005**, *249*, 545. (b) Du, M.; Li, C.-P.; Zhao, X.-J.; Yu, Q. *CrystEngComm* **2007**, *9*, 1011.

(9) (a) Lu, X. Q.; Jiang, J. J.; Chen, C. L.; Kang, B. S.; Su, C. Y. *Inorg. Chem.* **2005**, *44*, 4515. (b) Sivakumar, B. S.; Manimekalai, A. *Asian J. Chem.* **2009**, *21*, 5228. (c) Cui, F. Y.; Huang, K. L.; Xu, Y. Q.; Han, Z. G.; Liu, X.; Chi, Y. N.; Hu, C. W. *CrystEngComm* **2009**, *11*, 2757. (d) Manbeck, G. F.; Brennessel, W. W.; Evans, C. M.; Eisenberg, R. *Inorg. Chem.* **2010**, *49*, 2834.

(10) (a) Carlucci, L.; Ciani, G.; Garcia-Ruiz, J. M.; Moret, M.; Proserpio, D. M.; Rizzato, S. *Cryst. Growth Des.* **2009**, *9*, 5024. (b) Shin, D. M.; Lee, I. S.; Cho, D.; Chung, Y. K. *Inorg. Chem.* **2003**, *42*, 7722.

(11) (a) Montag, M.; Leitus, G.; Shimon, L. L. W.; Ben-David, Y.; Milstein, D. *Chem.—Eur. J.* **2007**, *13*, 9043. (b) Kumar, D. K.; Das, A.; Dastidar, P. *Cryst. Growth Des.* **2007**, *7*, 2096. (c) Du, M.; Wang, X. G.; Zhang, Z. H.; Tang, L. F.; Zhao, X. J. *CrystEngComm* **2006**, *8*, 788. (d) Lee, I. S.; MokShin, D.; Chung, Y. K. *Chem.—Eur. J.* **2004**, *10*, 3158.

(12) (a) Kanoo, P.; Gurunatha, K. L.; Maji, T. K. *Cryst. Growth Des.* **2009**, *9*, 4147. (b) Zheng, B.; Dong, H.; Bai, J. F.; Li, Y. Z.; Li, S. H.; Scheer, M. *J. Am. Chem. Soc.* **2008**, *130*, 7778. (c) Masaoka, S.; Tanaka, D.; Nakanishi, Y.; Kitagawa, S. *Angew. Chem., Int. Ed.* **2004**, *43*, 2530. (d) Forster, P. M.; Burbank, A. R.; Livage, C.; Férey, G.; Cheetham, A. K. *Chem. Commun.* **2004**, 368. (e) Tong, M. L.; Kitagawa, S.; Chang, H. C.; Ohba, M. *Chem. Commun.* **2004**, 418.

(13) (a) Du, M.; Li, C.-P.; Guo, J.-H. *CrystEngComm* **2009**, *11*, 1536. (b) Blake, A. J.; Champness, N. R.; Cooke, P. A.; Nicolson, J. E. B. *Chem. Commun.* **2000**, 665. (c) Du, M.; Guo, Y.-M.; Chen, S.-T.; Bu, X.-H.; Batten, S. R.; Ribas, J.; Kitagawa, S. *Inorg. Chem.* **2004**, *43*, 1287. (d) Chen, X.-D.; Mak, T. C. W. *Chem. Commun.* **2005**, 3529. (e) Gimeno, N.; Vilar, R. *Coord. Chem. Rev.* **2006**, *250*, 3161.

(14) (a) Long, L. S. *CrystEngComm* **2010**, *10*, 1354. (b) Li, C.-P.; Yu, Q.; Chen, J.; Du, M. *Cryst. Growth. Des.* **2010**, *10*, 2650. (c) Ma, L. F.; Wang, L. Y.; Wang, Y. Y.; Batten, S. R.; Wang, J. G. *Inorg. Chem.* **2009**, *48*, 915. (d) Wu, S. T.; Long, L. S.; Huang, R. B.; Zheng, L. S. *Cryst. Growth. Des.* **2007**, *7*, 1746. (e) Zhang, W. H.; Wang, Y. Y.; Lermontova, E. K.; Yang, G. P.; Liu, B.; Jin, J. C.; Dong, Z.; Shi, Q. Z. *Cryst. Growth. Des.* **2010**, *10*, 76. (f) Ou, G. C.; Su, C. Y.; Yao, J. H.; Lu, T. B. *Inorg. Chem. Commun.* **2005**, *8*, 421. (g) Lu, Y. B.; Wang, M. S.; Zhou, W. W.; Xu, G.; Guo, G. C.; Huang, J. S. *Inorg. Chem.* **2008**, *47*, 8935.

(15) (a) Li, X.; Xu, T. C.; Lu, H. B.; Ma, X. H.; Kai, L.; Guo, K. P.; Zhao, Y. H. *Protein Expression Purif.* **2010**, *69*, 16. (b) Kitamura, T.; Harada, T. *Green Chem.* **2001**, *3*, 252. (c) Di Cunto, F.; Topley, G.; Calautti, E.; Hsiao, J.; Ong, L.; Seth, P. K.; Dotto, G. P. *Science* **1998**, *280*, 1069. (d) Aida, K.; Foster, J. W. *Nature* **1962**, *196*, 672. (e) Hara, K.; Ichihara, Y.; Takahashi, K. *J. Biochem.* **1983**, *93*, 1435.

Scheme 1

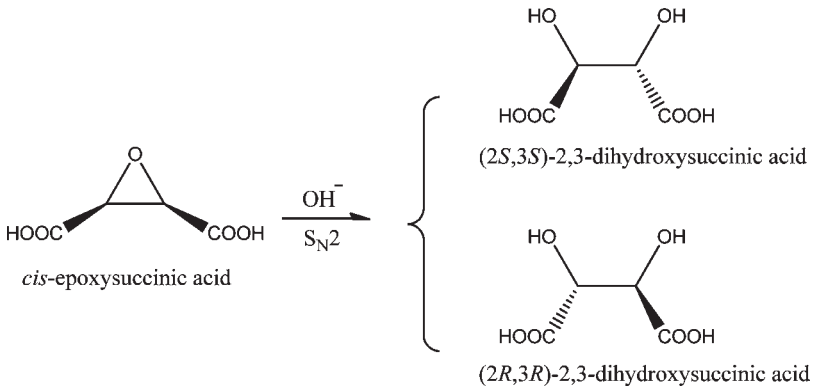

formation of polynuclear metal clusters because of its multiple coordination sites for both bridging and chelating functions (see Scheme 1).

Considering the aforementioned points, herein, we initially use *cis*-H_2ces as the building block to assemble with the Cu^{II} ion, generating two distinct crystalline products $\{[Cu(ces)(H_2O)_2](H_2O)_{0.5}\}_n$ (**1**) and $[Cu_{15}(dhs)_6(OH)_6(H_2O)_{10}](H_2O)_{20}$ (**2**), through delicately adjusting the pH conditions of the reaction system. These trials undoubtedly confirm the flexible nature of *cis*-H_2ces upon pH stimulus, which will be discussed in detail. Solid-state properties such as magnetism and thermal stability for both new materials have also been investigated and analyzed.

Experimental Section

Materials and Physical Measurements. All reagents and solvents were obtained commercially and used as received. Distilled water was used throughout. Fourier transform (FT) IR spectra (KBr pellets) were recorded in the range of 4000−400 cm^{-1} on a Tensor 27 OPUS (Bruker) FT-IR spectrometer. Elemental analyses (C and H) were performed on a Vario EL III elemental analyzer. Thermogravimetric analysis (TGA) experiments were carried out on a Perkin-Elmer Diamond SII thermal analyzer in the temperature range of 25−800 °C at a heating rate of 10 °C/min under N_2 atmosphere. Powder X-ray diffraction (PXRD) patterns were recorded on a Bruker D8 Advance diffractometer (Cu−Kα, λ = 1.54056 Å) at 40 kV and 30 mA, by using a Cu-target tube and a graphite monochromator. The powder samples were prepared by crushing the crystals, and the intensity data were recorded by continuous scan in a $2\theta/\theta$ mode from 3° to 80° with a step size of 0.02° and a scan speed of 2°/min. The calculated PXRD patterns were produced from the single-crystal diffraction data by using the PLATON software.[16] The pH values of the solution were determined by using a PHS-3C acidity meter. Magnetic measurements were carried out in the Unitat de Mesures Magnètiques (Universitat de Barcelona) on polycrystalline samples (ca. 30 mg) with a Quantum Design SQUID MPMS-XL magnetometer equipped with a 5 T magnet. Diamagnetic corrections were calculated using Pascal's constants, and an experimental correction for the sample holder was applied.

Preparation of the Complexes. $\{[Cu(ces)(H_2O)_2](H_2O)_{0.5}\}_n$ **(1).** To a methanol solution (2 mL) of *cis*-H_2ces (6.6 mg, 0.05 mmol), the pH value of which was adjusted to above about 9.5 by adding dropwise $NH_3 \cdot H_2O$ solution (pH = 12.0, at least 0.5 mL), was added a methanol (2 mL) solution of $Cu(ClO_4)_2 \cdot 6H_2O$ (18.6 mg, 0.05 mmol) with stirring for 5 min. And then, water (2 mL) was added to the resulting dark blue suspension with stirring, and the mixture was heated for 5 min and cooled to room temperature, affording a dark blue clear solution (initial pH = 7.40−8.28; see the Supporting Information, Table S3). Blue block crystals of **1** were obtained by slow evaporation of the solvents after about 1 day (final pH = 7.36−7.95; see Supporting Information, Table S3). Yield: 6.9 mg (58%, based on $Cu(ClO_4)_2 \cdot 6H_2O$). Anal. Calcd for $C_4H_7CuO_{7.5}$: C, 20.13; H, 2.96%. Found: C, 20.31; H, 3.07%. IR (cm^{-1}): 3346b, 3029w, 1622vs, 1458m, 1432m, 1399w, 1364w, 1349w, 1296w, 1240m, 1220m, 1130w, 1066m, 940m, 856w, 813m, 738w, 712m, 688w, 516w, 484w, 440w.

$[Cu_{15}(dhs)_6(OH)_6(H_2O)_{10}](H_2O)_{20}$ (2). To a methanol solution (2 mL) of *cis*-H_2ces (6.6 mg, 0.05 mmol), the pH value of which was adjusted to the range of about 9.1−9.5 by adding dropwise $NH_3 \cdot H_2O$ solution (pH = 12.0, 0.2−0.5 mL), was added a methanol (2 mL) solution of $Cu(ClO_4)_2 \cdot 6H_2O$ (18.6 mg, 0.05 mmol) with stirring for 5 min. And then, water (2 mL) was added to the resulting light blue suspension with stirring, and the mixture was heated for 5 min and cooled to room temperature, affording a light blue clear solution (initial pH = 6.58−7.32; see the Supporting Information, Table S4). Light blue block crystals of **2** were obtained by slow evaporation of the solvents after about 1 week (final pH = 6.31−7.13; see Supporting Information, Table S4). Yield: 5.1 mg (62%, based on $Cu(ClO_4)_2 \cdot 6H_2O$). Anal. Calcd for $C_{24}H_{78}Cu_{15}O_{72}$: C, 11.66; H, 3.18%. Found: C, 11.54; H, 3.31%. IR (cm^{-1}): 3417b, 1627vs, 1370s, 1316m, 1176w, 1149w, 1061m, 968m, 910w, 884w, 855w, 812m, 724w, 695w, 673w, 620w, 568m, 517w, 488w, 461w, 436w.

X-ray Crystallography. Single-crystal X-ray diffraction data for complexes **1** and **2** were collected on a Bruker Apex II CCD diffractometer at ambient temperature with Mo Kα radiation (λ = 0.71073 Å). A semiempirical absorption correction was applied using SADABS, and the program SAINT was used for integration of the diffraction profiles.[17] The structures were solved by direct methods using the SHELXS program of the SHELXTL package and refined with SHELXL.[18] The non-H atoms were modeled with anisotropic thermal parameters and refined by full-matrix least-squares methods on F^2. In general, C-bound hydrogen atoms were placed geometrically and refined as riding, whereas the O-bound hydrogen atoms were first located in difference Fourier maps, and then fixed in the calculated sites. Further details for crystallographic data and refinement conditions are listed in Table 1. Selected bond parameters and H-bonding geometries are shown in Supporting Information,

(16) Spek, A. L. *PLATON, A Multipurpose Crystallographic Tool*; Utrecht University: Utrecht, The Netherlands, 2005; available via http://www.cryst.chem.uu.nl/platon (for Unix) and http://www.chem.gla.ac.uk/~louis/software/platon/ (for MS Windows).

(17) *SAINT Software Reference Manual*; Bruker AXS: Madison, WI, 1998.

(18) Sheldrick, G. M. *SHELXTL NT Version 5.1. Program for Solution and Refinement of Crystal Structures*; University of Göttingen: Göttingen, Germany, 1997.

Tables S1 and S2 , respectively. CCDC-781598 and 781599 contain the supplementary crystallographic data for this paper. These data can be obtained free of charge from the Cambridge Crystallographic Data Centre via www.ccdc.cam.ac.uk/data_request/cif.

Results and Discussion

Synthesis and General Characterization. Complexes **1** and **2** were similarly synthesized by a direct self-assembly process of an equimolar Cu^{II}/H_2ces mixture at ambient conditions, but under different pH environments. In each case, the composition of the new material was determined by IR spectra, elemental analysis, and single crystal X-ray diffraction, and phase purity of the bulk sample was confirmed by PXRD technique (see Supporting Information, Figure S1). By comparison with the results of abundant parallel experiments (see Supporting Information, Tables S3−S5), it is confirmed that the pH value is a crucial factor in this synthetic system (see Scheme 2). That is, complexes **1** and **2** can be obtained from the similar reaction solutions, with the pH ranges of 7.40−8.28 and 6.58−7.32, respectively. After isolation of the crystalline product, the pH values of the resulting solution are 7.36−7.95 for **1** and 6.31−7.13 for **2**. Notably, the higher the pH value of the solution is, the darker its color is. Further experiments reveal that, if the reaction mixture is lower than about 6.5, light blue precipitates are obtained and the pH value of the remaining solution is 5.03−6.05 (see the Supporting Information, Table S5). Comparing its PXRD pattern and IR spectrum with those of **1**, **2**, and all reported Cu^{II}−H_4dhs complexes[19] (no Cu−H_2ces species is known so far), this precipitate represents an unknown complex (see Supporting Information, Figure S2). Additionally, complex **2** cannot be produced by directly assembling Cu^{II} with H_4dhs under similar conditions, indicating the advantage of in situ metal−ligand reaction in synthesizing new coordination systems.

Table 1. Crystallographic Data and Structural Refinement Summary for **1** and **2**

	1	**2**
chemical formula	$C_4H_7CuO_{7.5}$	$C_{24}H_{78}Cu_{15}O_{72}$
formula weight	238.64	2471.96
cryst system	orthorhombic	triclinic
space group	*Pbcn*	$P\bar{1}$
a (Å)	7.783(7)	10.934(1)
b (Å)	10.95(1)	11.519(1)
c (Å)	18.72(2)	14.902(2)
α (deg)	90	90.125(1)
β (deg)	90	93.914(1)
γ (deg)	90	112.645(1)
V (Å^3)	1497.2(1)	1721.3(4)
Z	8	1
ρ_{calcd} (g cm^{-3})	1.987	2.376
μ (cm^{-1})	2.744	4.653
F(000)	960	1233
parameters	115	502
R_{int}	0.0236	0.0263
R^a, $R_w{}^b$	0.0297, 0.0813	0.0370, 0.0834
GOF^c	1.074	1.029
residuals (e Å^{-3})	0.438, −0.576	0.892, −1.311

$^aR = \sum||F_o| - |F_c||/\sum|F_o|$. $^bR_w = [\sum[w(F_o^2 - F_c^2)^2]/\sum w(F_o^2)^2]^{1/2}$. ^{c}GOF $= \{\sum[w(F_o^2 - F_c^2)^2]/(n-p)\}^{1/2}$.

During the past decades, the complexes formed in the mixed solutions of Cu^{II} and H_4dhs under various pH environments, have been widely investigated and discussed.[19a] We noticed that the crystal structures of two Cu^{II} coordination polymers with H_4dhs under different pH conditions (a 2-D sheet complex $\{[Cu_2(H_2dhs)_2(H_2O)_2](H_2O)_4\}_n$[19b−f] and one 1-D chain species $\{[Cu(H_2dhs)](H_2O)_3\}_n$)[19b] have been determined (H_2dhs = partially deprotonated 2,3-dihydroxysuccinic acid with only the carboxyl groups ionized). In addition, a heterometal complex $\{[Na_2Cu(dhs)](H_2O)_5\}_n$ isolated from the basic solution was reported together with the magnetic properties, in which H_4dhs is completely deprotonated.[19g−i]

IR spectra of **1** and **2** show features attributable to compositions of the complexes. The broad bands centered at 3346 cm^{-1} for **1** and 3417 cm^{-1} for **2** indicate the O−H stretching of hydroxyl or water. For **1** and **2**, the characteristic bands of carboxylate groups appear in the region at 1622−1627 cm^{-1} for the antisymmetric stretching vibrations and at 1370−1432 cm^{-1} for the symmetric stretching vibrations. In addition, the absence of characteristic bands at about 1700 cm^{-1} rules out the presence of carboxyl group in **1** and **2**. Furthermore, the $\Delta\nu$ [$\nu_{as}(COO^-) - \nu_s(COO^-)$] values indicating the coordination modes of carboxylate are 164 and 190 cm^{-1} for **1** as well as 257 cm^{-1} for **2**, respectively, which are consistent with their solid structural features.

Scheme 2

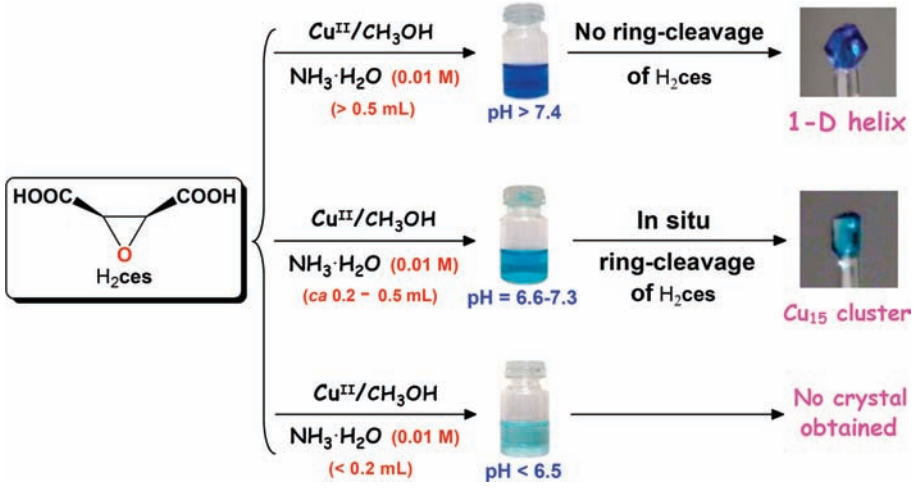

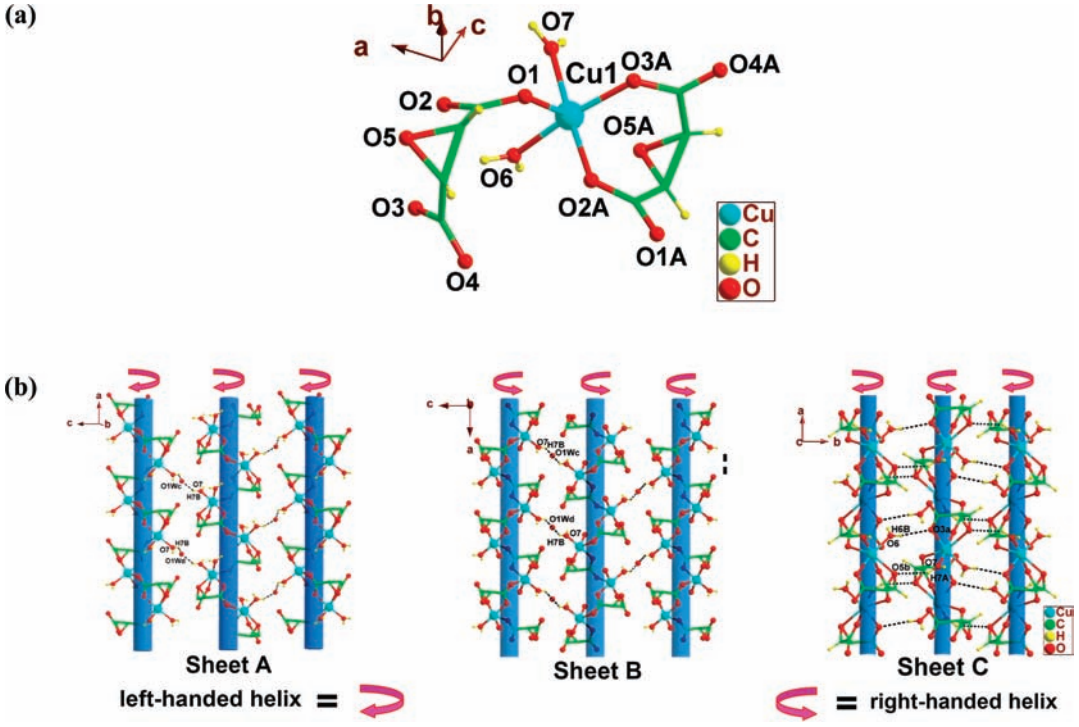

Figure 1. Views of **1**. (a) The coordination environment of Cu^{II} in the asymmetric unit of **1** (A = $x - 1/2, -y + 3/2, -z + 1$). (b) Two homochiral and one achiral 2-D sheets running parallel to *ac* and *ab* planes, respectively, showing the homochirality transfer (Sheet **A** and Sheet **B**) and opposite chirality transfer (Sheet **C**) through the interchain O−H···O hydrogen-bonding interactions (white dashed lines) between neighboring left- and/or right-handed helical chains.

Structural Description. $\{[Cu(ces)(H_2O)_2](H_2O)_{0.5}\}_n$ **(1).** Single-crystal X-ray diffraction reveals that the structure of **1** contains 1-D helical chain $[Cu(ces)(H_2O)_2]_n$ and lattice water molecule, with the interchain closest non-bonding Cu1···Cu1A separation of 5.181(3) Å (see Figure 1). The asymmetric unit has one Cu^{II} ion, one fully deprotonated *cis*-epoxysuccinate (ces) ligand, two water ligands, and half a lattice water molecule (see Figure 1a). In **1**, there is only one crystallographic independent Cu^{II} center that is penta-coordinated by three O atoms from two ces^{2-} ligands and two O atoms from two water molecules. Several parameters are often used to define the coordination geometry of a penta-coordinated metal ion, and the τ factor defined by Addison et al. is most common ($\tau = 0$ for regular square-pyramidal geometry and $\tau = 1$ for regular trigonal-bipyramidal geometry).[20] The τ value here is 0.10 for Cu^{II}, indicating an almost ideal square-pyramid environment. The Cu^{II} center deviates from the mean equatorial plane (O2A−O3A−O6−O7) toward the apical O1 atom by about 0.0769 Å. All bond lengths (1.997(3)−2.334(3) Å) and angles (84.3(1)−176.4(1)°) around Cu^{II} (see Supporting Information, Table S1) are comparable to those of the similar complexes in the literature.[21] Additionally, the adjacent Cu1···O5 distance is 2.472(3) Å, also indicating a weak interaction. In this structure, two carboxylate groups of each ces^{2-} take different coordination fashions with Cu^{II}, namely μ_2-η^1:η^1-*syn-anti* bridging and monodentate. In other words, each ces^{2-} ligand uses its two carboxylate groups in a *cis*-conformation on the oxirane ring to connect two Cu^{II} centers, forming two different left- and right-handed helical chains along the *a* axis with the period of 7.783(7) Å (see Figure 1b).[5a] The adjacent left- or right-handed helical chains are linked uniformly together by interchain O−H···O interactions (O7−H7B···O1W; see Supporting Information, Table S2),[14] running parallel to the *ac* plane, to afford two homochiral 2-D hydrogen-bonding sheets (denoted as Sheet **A** and Sheet **B**; see Figure 1b, left and middle). As such, the opposite chirality transfer is also observed in **1** between the alternately arranged left- and right-handed helical chains along the *b* axis, which results in the formation of an achiral 2-D hydrogen-bonding sheet, running along the *ab* plane, formed by interchain O−H···O interactions (O6−H6B···O3 and O7−H7A···O5; see Supporting Information, Table S2) (denoted as Sheet **C**; see Figure 1b, right). The chiral and achiral 2-D sheets mentioned above are further interlinked by intersheet O−H···O hydrogen bonds to generate an overall achiral 3-D hydrogen-bonding network (see Supporting Information, Figure S3).

(19) There are 24 crystal structures containing Cu^{II} and dhs, as indicated by a Cambridge Structural Database (CSD) search (release 5.31, November 2009, plus three updates). See: (a) Tapscott, R. E.; Belford, R. L.; Paul, I. C. *Coord. Chem. Rev.* **1969**, *4*, 323. (b) Prout, C. K.; Carruthers, J. R.; Rossotti, F. J. C. *J. Chem. Soc. A* **1971**, 3336. (c) Soylu, H. *Hacet. Bull. Nat. Sci. Eng.* **1982**, *11*, 61. (d) Jian, F.; Zhao, P.; Wang, Q. *J. Coord. Chem.* **2005**, *58*, 1133. (e) Pan, Y.-F.; Lu, W.-G. *J. Jiangxi Normal Univ.* (*Nat. Sci.*) **2006**, *30*, 209. (f) Zhang, D.; Templeton, D. H.; Zalkin, A. *ACA, Ser. 2* **1984**, *12*, 28. (g) Rajan, K. S.; Martell, A. E. *J. Inorg. Nucl. Chem.* **1967**, *29*, 463. (h) Missavage, R. J.; Belford, R. L.; Paul, I. C. *J. Coord. Chem.* **1972**, *2*, 145. (i) Belford, R. L.; Missavage, R. J.; Paul, I. C.; Chasteen, N. D.; Hatfield, W. E.; Villa, J. F. *Chem. Commun.* **1971**, 508.

(20) Addison, A. W.; Rao, T. N.; Reedijk, J.; van Rijn, J.; Verschoor, G. C. *J. Chem. Soc., Dalton Trans.* **1984**, 1349.

(21) (a) Wang, X.-Y.; Scancella, M.; Sevov, S. C. *Chem. Mater.* **2007**, *19*, 4506. (b) O'Keeffe, M.; Brese, N. E. *J. Am. Chem. Soc.* **1991**, *113*, 3226. (c) Liu, C.-S.; Wang, J.-J.; Yan, L.-F.; Chang, Z.; Bu, X.-H.; Sañudo, E. C.; Ribas, J. *Inorg. Chem.* **2007**, *46*, 6299.

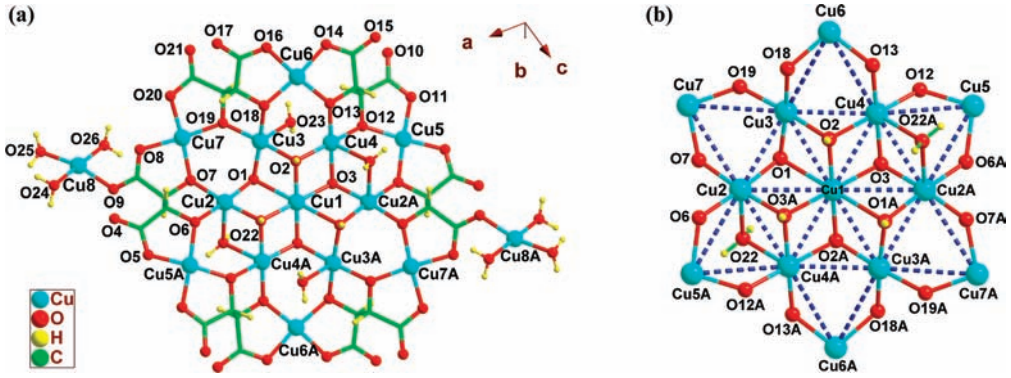

Figure 2. Views of **2**. (a) Molecular structure of the Cu_{15} cluster (symmetry code: A = $x+1, -y+1, -z+1$). (b) The simplified Cu_{13} structural core (see blue dashed lines) with a trinodal (6,5,2)-connected $(3^6.4^6.5^3)(3^4.4^3.5^2.6)_6(3)_6$ cluster topology (representing one central Cu^{II}, six interior-ring Cu^{II}, and six exterior-ring Cu^{II} nodes, respectively).

$[Cu_{15}(dhs)_6(OH)_6(H_2O)_{10}](H_2O)_{20}$ (2). Single-crystal X-ray diffraction analysis reveals that the structure of **2** consists of neutral isolated Cu_{15} nanoclusters $[Cu_{15}(dhs)_6(OH)_6(H_2O)_{10}]$ with an average diameter of about 1.5 nm (see Figure 2a) and numerous lattice water molecules. The asymmetric unit consists of seven and a half crystallographically unique Cu^{II} centers with the closest nonbonding Cu1···Cu4 separation of 3.0483(6) Å, three fully deprotonated dhs^{4-} components (two (2*S*,3*S*)-dhs related to C2/C3 and C6/C7 atoms and one (2*R*,3*R*)-dhs related to C10/C11 atoms), three μ_3-OH^- anions, five water ligands, and ten lattice water molecules. All Cu^{II} centers are almost coplanar, from the central Cu1 ion to the interior six-membered Cu^{II} ring (Cu2−Cu3−Cu4−Cu2A−Cu3A−Cu4A), the exterior six-membered Cu^{II} ring (Cu5−Cu6−Cu7−Cu5A−Cu6A−Cu7A), and the terminal Cu8 and Cu8A ions in each pentadeca-nuclear unit of $[Cu_{15}(dhs)_6(OH)_6(H_2O)_{10}]$. Three types of coordination environments are observed for these Cu^{II} centers. The first type (Cu1) is a six-coordinated elongated octahedral geometry with four μ_3-OH^- anions building the equatorial plane (Cu−O = 1.995(3)−2.026(3) Å) and the other two μ_3-OH^- groups standing on the axial sites (Cu1−O1 = 2.347(3) Å). The second type (Cu2, Cu3, and Cu4 in the interior six-membered Cu^{II} ring) resides in a penta-coordinated square pyramid, in which the basal plane is defined by two μ_3-OH^- anions (Cu−O = 1.940(3)−1.995(3) Å) and two μ_2-O^- groups in a dhs^{4-} ligand (Cu−O = 1.924(3)−1.981(3) Å), while the apical sites are occupied by one μ_2-H_2O ligand (Cu−O = 2.294(4)−2.416(4) Å). Here, the τ values are 0.01 for Cu2, 0.02 for Cu3, and 0.11 for Cu4, indicating their nearly ideal square-pyramidal coordination geometries.[18] The third type (Cu5, Cu6, and Cu7 in the exterior six-membered Cu^{II} ring) has two μ_2-O^- groups (Cu−O = 1.911(4)−1.949(3) Å) and two carboxylate oxygen atoms (Cu−O = 1.930(4)−1.959(4) Å) from two different dhs^{4-} ligands in the square planar coordination environment. As such, the Cu8 and Cu8A centers in the terminal positions of each pentadeca-nuclear unit are also four-coordinated, which however, are completed by one carboxylate O atom (Cu−O = 2.012(4) Å) and three water ligands (Cu−O = 1.971(6)−2.021(5) Å). In other words, the pentadeca-Cu^{II} cluster of **2** is formed by one central $Cu^{II}O_6$ octahedron, six interior-ring $Cu^{II}O_5$ square pyramids, six exterior-ring $Cu^{II}O_4$ planar quadrilaterals, and two terminal $Cu^{II}O_4$ planar quadrilaterals. In addition, six interior $Cu^{II}O_5$ and six exterior $Cu^{II}O_4$ centers constitute two centrosymmetric hexagon-like Cu_6 clusters $[Cu_6O_{12}(OH)_6(H_2O)_4]$ and $[Cu_6O_{24}]$. With the long Cu···O lengths excluded, all the remaining Cu−O lengths (1.911(4)−2.416(4) Å) and bond angles (74.0(1)−180.0(2)°) around each Cu^{II} in **2** are quite typical for Cu^{II}, with the coordination geometries of axial elongation (see Supporting Information, Table S1) and significant Jahn−Teller effect.

A better insight into the $[Cu_{15}(dhs)_6(OH)_6(H_2O)_{10}]$ cluster can be achieved by the application of a new topological approach for polynuclear clusters proposed by Powell and Kostakis,[22] in which each metal center of a cluster can be designated as a straightforward "node" and the binding O- and/or N- heteroatoms then as the "linker". Following this lead, one can define a cluster in terms of the connectivity of its vertices by using the approach adopted by O'Keeffe et al.[23] In this way, if taking no account of two terminal $Cu^{II}O_4$ planar quadrilaterals (Cu8 and Cu8A), the resulting Cu_{13} cluster can be described as a trinodal (6,5,2)-connected $(3^6.4^6.5^3)(3^4.4^3.5^2.6)_6(3)_6$ cluster topology (representing one central Cu^{II}, six interior-ring Cu^{II}, and six exterior-ring Cu^{II} nodes, respectively) (see Figure 2b). According to the latest version of Cambridge Crystallographic Database[19] and Inorganic Crystal Structure Database,[24] such a coplanar Cu_{15} cluster has not been reported so far, not only in coordination chemistry[6] but also in polyoxometalate (POM) chemistry.[25]

Each isolated Cu_{15} cluster, in turn, is interlinked to its nearest eight Cu_{15} neighbors to build a higher-dimensional

(22) Kostakis, G. E.; Powell, A. K. *Coord. Chem. Rev.* **2009**, *253*, 2686.
(23) (a) Wells, A. F. *Three-Dimensional Nets and Polyhedra*; Wiley-Interscience: New York, 1977. (b) Wells, A. F. *Further Studies of Three-Dimensional Nets*, ACA Monograph No. 8; American Crystallographic Association, 1979. (c) O'Keeffe, M.; Hyde, B. G. *Crystal Structures I. Patterns and Symmetry*; Mineralogical Society of America: Washington, DC, 1996. (d) Barnett, S. A.; Champness, N. R. *Coord. Chem. Rev.* **2003**, *246*, 145. (e) Carlucci, L.; Ciani, G.; Proserpio, D. M. *Coord. Chem. Rev.* **2003**, *246*, 247. (f) Batten, S. R.; Neville, S. M.; Turner, D. R. *Coordination Polymers: Design, Analysis and Application*; Royal Society of Chemistry (RSC) Publishing: Cambridge, U.K., 2008. (g) O'Keeffe, M.; Peskov, M. A.; Ramsden, S. J.; Yaghi, O. M. *Acc. Chem. Res.* **2008**, *41*, 1782.
(24) http://icsdweb.fiz-karlsruhe.de.
(25) (a) Zhao, J.-W.; Wang, C.-M.; Zhang, J.; Zheng, S.-T.; Yang, G.-Y. *Chem.—Eur. J.* **2008**, *14*, 9223. (b) Zheng, S.-T.; Yuan, D.-Q.; Zhang, J.; Yang, G.-Y. *Inorg. Chem.* **2007**, *46*, 4569.

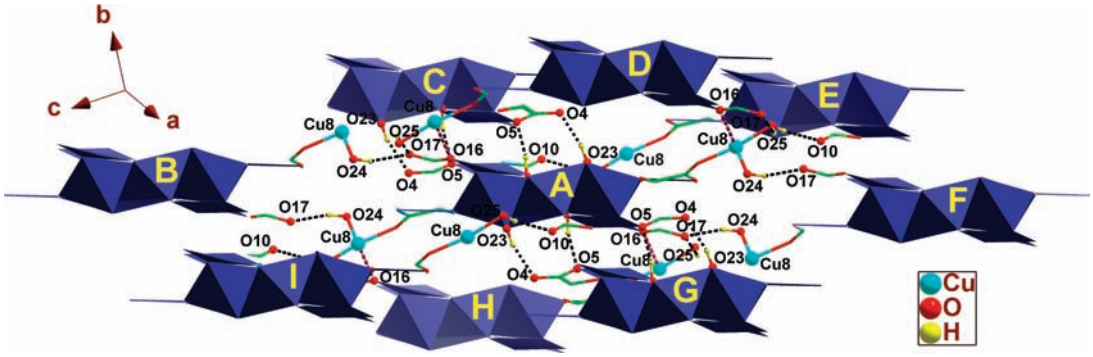

Figure 3. Portion view of the 3-D supramolecular structure of **2**, showing how each isolated Cu_{15} cluster (blue polyhedral representation A−I) is interlinked to its nearest eight pentadeca-Cu^{II} neighbors through intermolecular O−H···O hydrogen-bonding (black dashed lines) and weak Cu···O (violet dashed lines) interactions, namely, O24−H6W···O17 between A and B as well as A and F, O23−H4W···O4 and O3−H3D···O5 between A and C as well as A and G, O25−H7W···O10 between A and E as well as A and I, and O25−H8W···O17 and Cu8···O16 interactions between A and D as well as A and H (please see Supporting Information, Table S2 for detailed H-bonding parameters). Only oxygen and hydrogen atoms involved in the interactions are shown for clarity.

supramolecular framework through weak Cu8···O16 (2.6821(4) Å) interactions and intermolecular O−H···O bonds between the dhs^{4-} ligands and coordinated water molecules (see Figure 3 and Supporting Information, Table S2).

In addition, the adjacent $[Cu_{15}(dhs)_6(OH)_6(H_2O)_{10}]$ units are assembled into three different 2-D sheets, being parallel to the crystallographic $(1\bar{1}1)$, $(1\bar{1}0)$, and (001) planes, respectively, by co-effects of intermolecular Cu8···O16 and O−H···O interactions mentioned above. Analysis of the network topology provides a convenient tool in understanding the complicated crystal structures of crystalline materials, especially for coordination polymers and hydrogen-bonding networks.[23] To better understand the connectivity between the $[Cu_{15}(dhs)_6(OH)_6(H_2O)_{10}]$ units, the 3-D supramolecular architecture in **2** can be simplified to a **hex** topological network (see Figure 4 and the Supporting Information, Figure S4) with the Schläfli symbol of $(3^6.4^{18}.5^3.6)$, by considering each Cu_{15} cluster as a uniform 8-connected node. All uncoordinated water molecules lie in the cavity of such a host network and form multiple O−H···O hydrogen-bonding interactions between themselves and/or with the dhs^{4-} ligands (see Supporting Information, Table S2).

Effect of pH Condition and in Situ Ligand Reaction. Since the only difference for the synthetic condition of complexes **1** and **2** is the pH value of the reaction solution, it is clear that the type of crystalline products formed depends on its pH parameter, which interestingly, will result in the in situ metal−ligand formation as demonstrated above. As for **1**, the higher pH value (>7.40) favors to keep the ces^{2-} backbone intact, and the ratio of Cu^{II}/ces^{2-} is 1:1. Correspondingly, a 1-D helical chain motif is afforded. As for **2**, the middle pH value (6.58−7.32) facilitates the in situ reaction of H_2ces to H_4dhs during the coordination-driven assembling process. Significantly, two isomers (2*S*,3*S*)- and (2*R*,3*R*)-dhs with a ratio of 2:1 are formed in this course from the S_N2 ring-cleavage reaction, which interlink the Cu^{II} centers into a neutral isolated Cu_{15} nanocluster, with the aid of hydroxyl anions. If the pH value becomes lower (< about 6.5), an unknown light blue precipitate will be produced. Although we have tried many times, no suitable single crystals for X-ray diffraction could be obtained.

Magnetic Properties. Magnetic susceptibility data for **1** were measured at an applied field of 1 T between 300 and 2 K, and at an applied field of 500 Oe between 30 and 2 K. No field dependence of the susceptibility was observed; thus, for clarity only the data at 1 T is shown in Figure 5 as χ and χT versus T plots, and in Figure 6 as a Curie plot. The susceptibility has a maximum at $T = 6$ K, indicating the onset of the antiferromagnetic state. The experimental data were fitted according to the Bonner−Fisher equation (see eq 1)[26] for 1-D $S = 1/2$ systems with the g value of 2.0 and the best fitting parameter $J = -6.68$ cm^{-1}.

$$\chi = g^2\mu_B{}^2N/kT[A + Bx + Cx^2]/[1 + Dx + Ex^2 + Fx^3] \quad (1)$$

$$A = 0.25,\ B = 0.149445,\ C = 0.30094,$$
$$D = 1.9862,\ E = 0.68854,\ F = 6.0626,\ x = J/kT$$

The calculated data are shown in Figure 5 as the solid line. The exchange parameter obtained is in good agreement with that obtained from the Curie−Weiss fitting of the high temperature data ($T > 25$ K, $C = 0.46$ cm^3 mol^{-1}, and $\Theta = -10.67$ K), using the mean-field approximation (see eq 2)[27] and affording the exchange parameter $J = -7.3$ cm^{-1}. The linear response of the magnetization versus field at 2 K observed for **1** confirms the $S = 0$ ground state (see Supporting Information, Figure S5).

$$\chi = Ng^2\mu_B{}^2S(S+1)/3k(T-\theta)$$
$$\theta = 2S(S+1)zJ'/3k \quad (2)$$

Magnetic susceptibility data were collected for a crushed crystalline sample of **2** in the 2−300 K temperature range and at applied fields of 500 G and 1.0 T. The data were not field dependent; thus, only the 1.0 T data are shown. A χT versus T plot per Cu_{15} unit is shown in Figure 7. The χT product has a value of 4.3 cm^3 K mol^{-1} at 300 K, below the expected value of 5.6 cm^3 K mol^{-1} for 15 isolated Cu^{II} ions with $g = 2.0$ and $S = 1/2$. As the temperature decreases so does the χT product, indicating

(26) Estes, W. E.; Gavel, D. P.; Hatfield, W. E.; Hodgson., D. J. *Inorg. Chem.* **1978**, *17*, 1415.
(27) Carlin, R. L. *Magnetochemistry*; Springer-Verlag: New York, 1986; p 12.

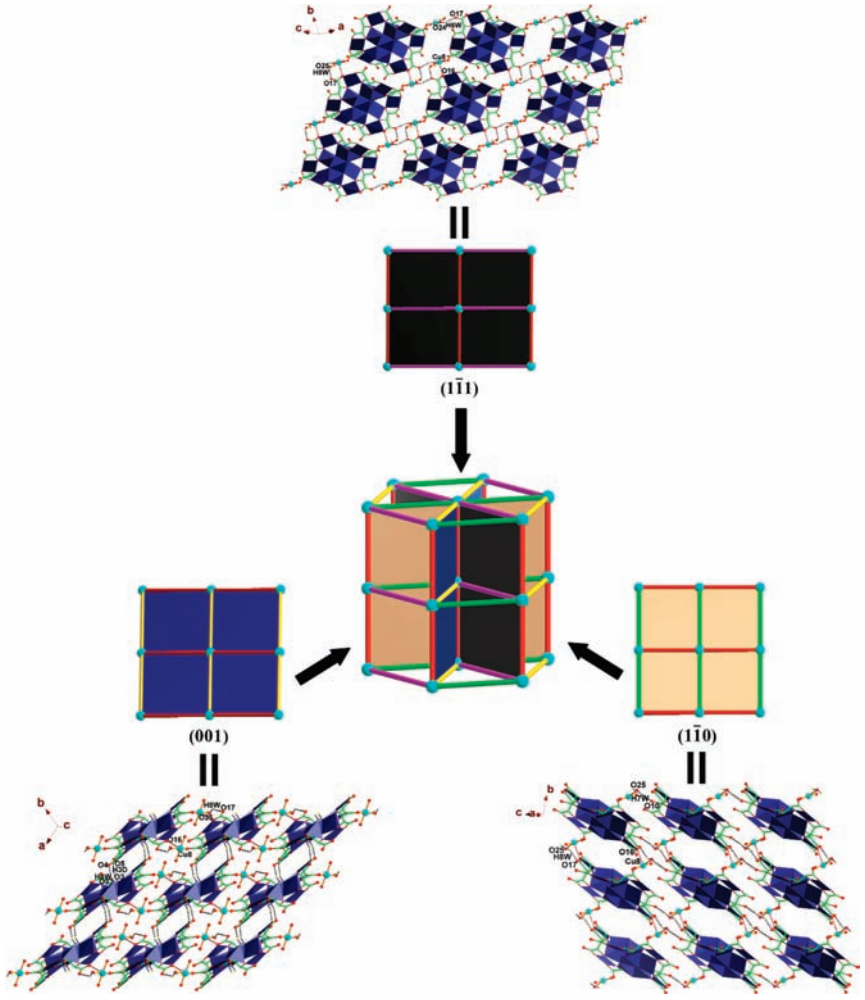

Figure 4. Detailed illustration of the 8-connected 3-D hydrogen-bonding ($3^6.4^{18}.5^3.6$) **hex** net in **2**, showing three types of 2-D packing sheets in different crystallographic directions.

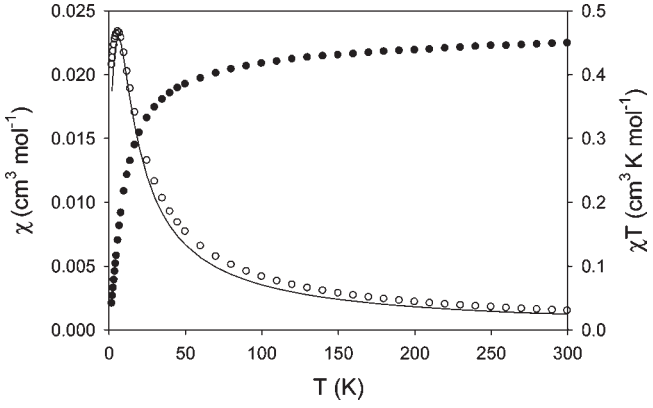

Figure 5. Susceptibility plot for **1** (hollow circles, left axis) and χT versus T plot (black circles, right axis). The solid line is the best fitting of the experimental data using the Bonner−Fisher equation (see text for fitting parameters).

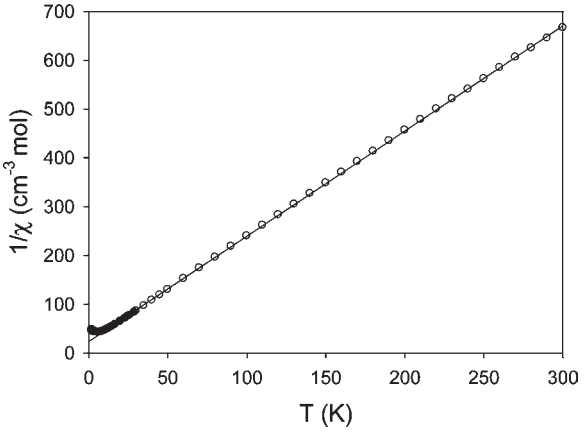

Figure 6. Curie−Weiss plot for **1**. The solid line is the best fitting of the high-temperature data using the Curie−Weiss law (see the text for the fitting parameters).

antiferromagnetic interactions. A minimum is achieved at 15 K, and below this temperature the χT product rises again to a value of 1.7 at 2 K, indicating the population of a non-zero spin ground state. A Curie plot is shown in Figure 8. It can be clearly divided in two distinct regions, a high temperature (HT) region from 300 to 150 K, and a low temperature (LT) region from 2 to 25 K. **2** is formed by Cu_{15} units that are linked to the nearest neighbors to form a 3-D network by weak interactions. Because of the structural complexity of **2**, the Cu_{15} unit will be considered as a magnetically isolated cluster with weak interactions to its neighbors. Even so, the complexity and large numbers of pairwise interactions of **2** preclude the use of the Kambe approach to find an analytical solution to

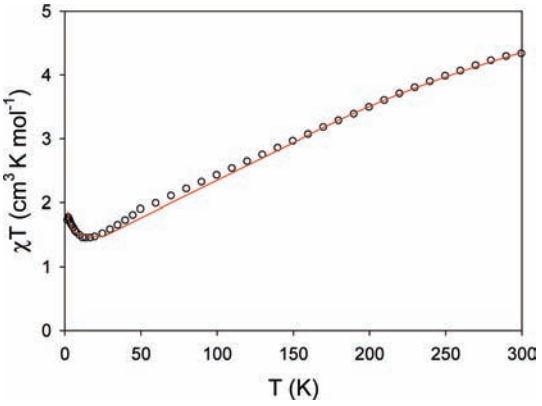

Figure 7. χT versus T plot for **2** at 1.0 T applied magnetic field. The red solid line is the best fitting to the experimental data (see text for fitting parameters).

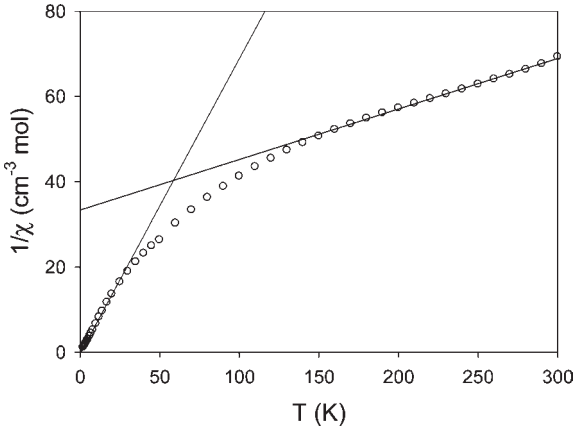

Figure 8. Curie plot for **2**. The solid lines are the best fit to the Curie–Weiss law in the two distinct temperature regions (see text for fitting parameters).

obtain the pairwise exchange parameters or the exact solution of the Hamiltonian to obtain the energies of the spin states. Instead, the complex **2** can be treated as a central Cu_{13} core where the antiferromagnetic interactions related to the Cu–O–Cu angles dominate and lead to $S = 1/2$. The full matrix diagonalization of the Hamiltonian of the Cu_{13} unit is in fact possible using the software SpinMart[28] which performs a simulation of the magnetic data. For various combinations of values of the pairwise exchange constants, all of them antiferromagnetic, a spin ground state of $S = 1/2$ is obtained. The Hamiltonian used is

$$\hat{H} = \sum_{i,j} J\vec{S}_i \bullet \vec{S}_j - g\mu_B H \sum_i \vec{S}_i$$

and the spin system used can be found in the Supporting Information, Figure S6. This $S = 1/2$ Cu_{13} core is linked to two Cu^{II} ions, Cu8 and the symmetry related Cu8A, by *syn,anti*-carboxylato groups (see Figure 2a), which result in the expected weak ferromagnetic coupling and thus $S = 3/2$ for **2**. Average values of all the contributing interactions can be obtained using the Curie–Weiss law; the best fittings are shown in Figure 8 as solid line. The obtained parameters are $C_{HT} = 8.4$ cm^{-3} mol, $\Theta_{HT} = -280$ K, $C_{LT} = 1.4$ cm^{-3} mol, and $\Theta_{LT} = 0.4$ K. The Weiss constants obtained indicate a dominant antiferromagnetic interaction in the HT region and a dominant ferromagnetic interaction at the low temperature region, leading to $S = 3/2$. The χT product calculated using these parameters shows an excellent agreement with the experimental data, as shown in Figure 7. The magnetization versus field behavior at 2 K was also studied, as shown in the Supporting Information, Figure S7. Saturation is reached near a value of 2.9, and the data follows the Brillouin curve for an $S = 3/2$ with $g = 2.0$, in agreement with the susceptibility data. This can be easily understood according to the above structural analysis of complex **2**.

Thermogravimetric Analysis. To examine the thermal stability of **1** and **2**, thermogravimetric analysis (TGA) experiments were performed by heating the corresponding crystalline samples (see the Supporting Information, Figure S8). The TGA curve of **1** shows the first weight loss of 3.69% between 140 and 160 °C (peaking at 158 °C), corresponding to the loss of one lattice water molecule (calcd: 3.78%). The second weight loss of 7.68% in the range of 160–190 °C is in accordance with the loss of two coordinated water molecules per unit cell (calcd: 7.55%). Then, complex **1** starts to quickly decompose and yields the final residue CuO (obsd: 32.95% and calcd: 33.33%) with two consecutive steps of weight loss (peaking at 208 and 235 °C). The TGA curve of **2** reveals that the first weight loss of 7.48% in the temperature region of 25–86 °C (peaking at 65 °C) corresponds to the expulsion of lattice water molecules (calcd: 7.29%). The residual component starts to decompose beyond 86 °C with a series of weight losses (peaking at 204, 226, and 238 °C). The final species holds a weight of 47.47% of the total sample, and seems to be CuO (calcd: 48.27%).

Conclusions and Perspectives

In summary, we report here two novel coordination assemblies generated from *cis*-epoxysuccinic acid and $Cu(ClO_4)_2$ under different pH conditions, including a 1-D helical motif and a neutral isolated Cu_{15} nanocluster. It is confirmed that the pH value of reaction media will have a significant effect on the conformation of the organic ligands involved in the final coordination products (*cis*-epoxysuccinate vs dihydroxysuccinate) with distinct structural architectures and solid-state properties. These interesting results prompt us to further study more related metallosupramolecular systems with *cis*-epoxysuccinic acid and other metal ions and/or organic co-ligands under different external conditions.

Acknowledgment. This work was supported by the National Natural Science Fund of China (Grant Nos. 20801049 and 20771095), the Startup Fund for PhDs of Natural Scientific Research of Zhengzhou University of Light Industry (Grant No. 2007BSJJ001 to C.S.L.), Henan Outstanding Youth Science Fund (to C.S.L.), and Tianjin Normal University (to M.D.). E.C.S. acknowledges the financial support from the Spanish Government (Grant CTQ2009-06959 and Ramón y Cajal contract). We also thank Mr. X.-G. Yang for helping us to analyze the topological structure of complex **2**.

(28) Engelhardt, L.; Rainey, C. *Fit Mart Simulation software*; Francis Marion University: Florence, SC

Supporting Information Available: Selected bond lengths and angles for **1** and **2** (Table S1), important H-bonding geometries for **1** and **2** (Table S2), the pH parameters during the assembling processes of **1** (Table S3), **2** (Table S4), and the light blue precipitate (Table S5), PXRD patterns of **1** and **2** (Figure S1), comparison of IR spectra and PXRD patterns of **1**, **2** and the light blue precipitate (Figure S2), the achiral 3-D hydrogen-bonding network in **1** (Figure S3), schematic representation of the **hex** topological network in **2** (Figure S4), magnetization versus field behavior of **1** (Figure S5) and **2** (Figure S7) at 2 K, the spin system used for the full matrix diagonalization in **2** (Figure S6), and TGA plots of **1** and **2** (Figure S8). This material is available free of charge via the Internet at http://pubs.acs.org.